

# MagTex: Machine-Knitted Magnetoactive Textiles for Bidirectional Human-Machine Interface

Sen Zhang

Electrical and Computer Engineering  
University of Washington  
Seattle, Washington, USA  
szhang66@uw.edu

Jazlin Taylor

Electrical & Computer Engineering  
University of Washington  
Seattle, Washington, USA  
jazlin@uw.edu

Yuxuan Miao

Electrical & Computer Engineering  
University of Washington  
Seattle, Washington, USA  
ymiao6@uw.edu

Yiyue Luo

Electrical & Computer Engineering  
University of Washington  
Seattle, Washington, USA  
yiyueluo@uw.edu



**Figure 1:** A, MagTex is a bidirectional human-machine interface. It consists of a magnetoactive fiber and machine-knitted electromagnet, enabling the co-located sensing and haptic capabilities. We demonstrate applications of MagTex: B, a wearable soft controller for a video game, C, a Braille character display for visually impaired users, and D, a closed-loop interface for running speed monitoring and real-time feedback.

## Abstract

Bidirectional human-machine interfaces (HMIs) provide both sensing and haptic feedback, enabling responsive and intuitive interactions across a wide range of applications, including assistive technologies, robotics, and augmented/virtual reality (AR/VR). In this paper, we present MagTex, a bidirectional HMI platform realized through digitally machine-knitted magnetoactive textiles. MagTex integrates sensing and haptic feedback within a single, wearable interface by embedding soft magnetoactive fibers into machine-knitted electromagnets. MagTex delivers localized vibrotactile feedback through the galvanomagnetic effect and achieves motion sensing via electromagnetic induction. We describe the

digital fabrication workflow, material characterization, circuits implementation, and system integration in detail. A user study confirms both the perceptibility of the haptic feedback and the thermal property of the textile system. We demonstrate the capability of MagTex through three application scenarios: a wireless smart sleeve for game control, a tactile Braille display glove, and a closed-loop smart knee brace for real-time running feedback. Overall, MagTex offers a soft, scalable, and compact solution for bidirectional HMIs.

## CCS Concepts

- Human-centered computing → Human computer interaction (HCI).

## Keywords

E-textile; wearable human-machine interface; haptics feedback; sensing; magnetoactive fiber

## ACM Reference Format:

Sen Zhang, Yuxuan Miao, Jazlin Taylor, and Yiyue Luo. 2025. MagTex: Machine-Knitted Magnetoactive Textiles for Bidirectional Human-Machine



This work is licensed under a Creative Commons Attribution 4.0 International License.  
UIST '25, Busan, Republic of Korea  
© 2025 Copyright held by the owner/author(s).  
ACM ISBN 979-8-4007-2037-6/25/09  
<https://doi.org/10.1145/3746059.3747648>

Interface. In *The 38th Annual ACM Symposium on User Interface Software and Technology (UIST '25), September 28–October 01, 2025, Busan, Republic of Korea*. ACM, New York, NY, USA, 15 pages. <https://doi.org/10.1145/3746059.3747648>

## 1 Introduction

Human–machine interfaces (HMIs) are evolving toward systems that enable both sensing and haptic feedback to support more intuitive, responsive, and immersive user experiences in domains such as healthcare, robotics, and augmented/virtual reality (AR/VR) [23, 31, 44]. Recent advances in soft electronics have propelled this transformation by moving interaction away from rigid, handheld devices toward soft, wearable platforms [38, 43, 50]. These soft interfaces conform to the human body and allow for more natural movement and interaction.

Among diverse soft interfaces, textiles are inherently breathable, flexible, and comfortable, making them ideal candidates for seamless and user-friendly wearable interfaces. Smart textiles, fabrics integrated with electronic functionalities, are capable of supporting a wide range of human–machine interactions while maintaining the form factor of everyday clothing [6, 25]. Sensing is typically achieved through resistive [2], capacitive [11], or electromagnetic induction [35], while haptic feedback is delivered using actuators such as dielectric elastomer actuators (DEAs) [52], magnetic actuators [10], or pneumatic artificial muscles (PAMs) [34], which often lack intrinsic sensing capabilities. However, the majority of current smart textiles implement sensing and haptic functionalities as separate components, constrained by the trade-off between compact form factor and the complexity of functional integration.

Recent work has explored the integration of magnetic actuation and sensing within a single platform [26, 28]. While these systems effectively combine permanent magnets and electromagnetic coils, achieving this integration typically relies on rigid components, resulting in bulky form factors that remain challenging to adapt for wearable or scalable use. Thus, there is a clear need for soft, fully textile-based HMIs that support bidirectional interaction, both sensing and haptic feedback, within compact, conformable, and large spatial coverage designs.

To this end, we introduce MagTex, a novel machine-knitted magnetoactive textile for bidirectional human–machine interactions. MagTex integrates both sensing and haptic functions into a single textile unit by embedding soft magnetoactive fibers within machine-knitted electromagnets. MagTex enables seamless bidirectional interaction by converting motion into electrical signals for sensing and electrical signals into mechanical vibrations for haptic feedback. This is achieved within a single unit, without relying on external modules or rigid hardware. Our circuit supports switching between the sensing and haptic functions at up to 100 Hz, with a low latency of 10 ms.

Our system is fabricated using digital fiber extrusion and computerized flatbed knitting, allowing scalable, customizable, and spatial coverage interfaces that preserve textile softness and breathability. A customized portable wireless circuit is developed to support both sensing and haptic modes in real time, enabling seamless communication with computers or other digital platforms. MagTex can sense user-generated mechanical interactions, such as tapping

or scratching motions, while simultaneously delivering targeted haptic feedback across different locations on the body.

We validate the multifunctionality of MagTex through comprehensive material, sensing, and haptics characterization. Further, we demonstrate its three proof-of-concept applications: a wireless smart sleeve that functions as a video game controller through gesture recognition, a Braille display glove providing localized haptic output for non-visual communication, and a closed-loop smart knee brace that monitors running speed and delivers real-time feedback via a connected haptic glove. Together, these contributions establish MagTex as a promising platform for scalable, fabric-based, bidirectional HMIs suited for interactive, wearable technologies.

The main contributions of this paper are:

- We design and fabricate MagTex, a bidirectional HMI using customized magnetoactive fibers and machine-knitted electromagnets.
- We develop a portable, wireless circuit that interfaces MagTex with external systems for real-time sensing and haptic feedback.
- We characterize the magnetic, mechanical, sensing, thermal, and haptic properties of MagTex and optimize the parameters for both sensing and haptic performance.
- We demonstrate MagTex in example applications, including a wireless soft controller for video games, a tactile Braille display glove, and a closed-loop running speed monitor using a smart knee brace and haptic glove.

## 2 related work

Our work is based on prior research in wearable sensors and actuators. This section provides a brief review of existing literature on textile-based sensors and actuators, as well as their integration in interactive systems.

### 2.1 Textile-Based Interactive Interface

In recent years, textiles have received increasing attention as a promising platform for building wearable electronic systems. By directly embedding functional electronic components such as sensors, actuators, and circuits into textile structures, wearable devices with excellent interactivity have been vigorously developed. The integration of textiles and electronics not only preserves the original softness, fitness, and breathability of fabrics, but also enhances the comfort and practicality of devices in daily use scenarios, providing strong support for the practicality and portability of wearable technology.

*Sensing.* Researchers have developed various forms of sensing systems, such as gloves [29, 40], finger caps [1, 55], and wearable accessories [4, 28]. Commonly used sensing mechanisms include resistive, capacitive, electromagnetic, and triboelectric. Resistive sensors, such as those developed by Lee et al. [19, 46] using conductive yarns to detect pressure or deformation, often suffer from unstable electrical contact points. These loose contacts can lead to inconsistent resistance measurements under repeated or identical mechanical stimuli. Zhang et al. [48] proposed a graphene-coated fabric that can change the contact resistance of its nano network

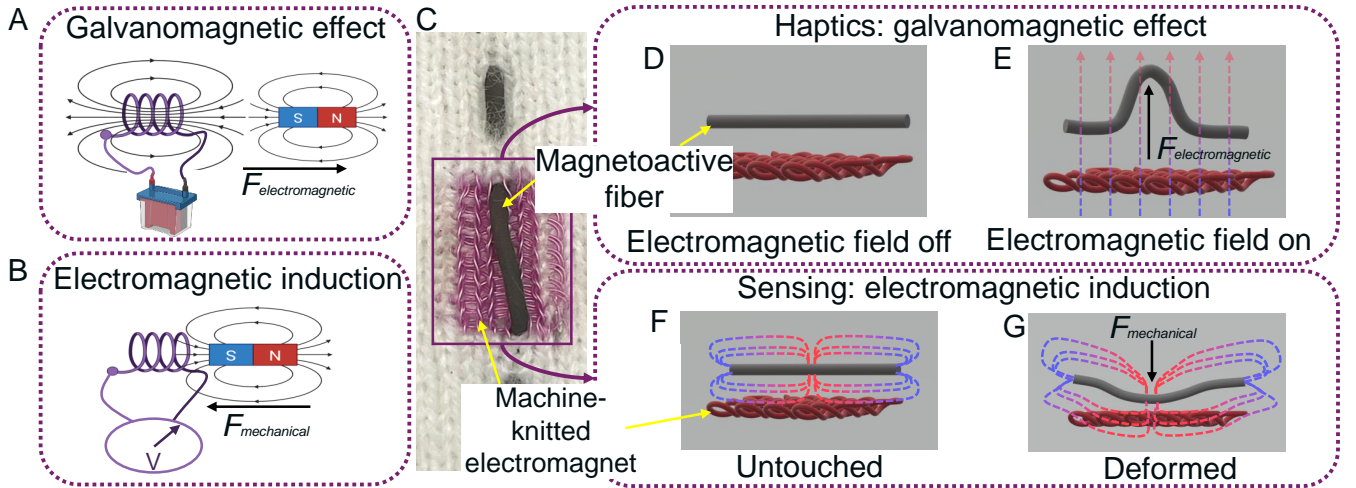


**Figure 2:** System overview of MagTex. **A**, Illustration of the galvanomagnetic effect between a powered solenoid and a magnet. **B**, Electromagnetic induction occurring in the coil due to the motion of a nearby magnet. **C**, A MagTex unit composed of a magnetoactive fiber integrated with a machine-knitted electromagnetic coil. **D–E**, Working principle of MagTex haptic function, where AC induces vibration via the galvanomagnetic effect. **F–G**, Working principle of MagTex sensing function, where magnetoactive fiber motion induces an electromotive force in the machine-knitted electromagnet.

during deformation. However, this method exhibits significant sensitivity variation across different pressure ranges and faces nonlinear challenges. Capacitive sensors have good sensitivity and scalability in array configurations. Keum et al. [15] demonstrated a dual electrode fabric integrated pressure sensor for multi-point detection applications. Stretchable capacitive sensors [47] provide continuous deformation sensing but often suffer from poor adhesion between their microstructure dielectric layers and electrodes. This results in unstable air gaps and dielectric constants that cause performance fluctuations across batches or devices. Electromagnetic sensors can achieve non-contact position and posture sensing through the interaction between the coils embedded in fabrics and external magnetic fields. For example, Hall effect textile sensors [33] allow users to slide their fingers with small magnets into the sensing area to control the device. Lugoda et al. [24] integrated giant magnetoresistance (GMR) sensors into fabric sleeves, achieving motion control in virtual reality environments. Triboelectric nanogenerators (TENGs), which convert mechanical motion into electrical signals via contact electrification and electrostatic induction, are also widely used for motion sensing in wearable systems [7, 8, 13, 21]. They are self-powered and well-suited for detecting tactile interactions, gesture dynamics, and deformation without the need for external power supplies.

These sensing systems, characterized by one-way input acquisition, have achieved significant results in motion capture and posture recognition. Building upon these advances, our proposed system integrates both sensing and haptic feedback functions on a single textile platform. By knitting magnet wire into flexible textiles as electromagnet and sewing highly stretchable magnetoactive fibers, the system achieves bidirectional interaction in a unified structure, greatly enriching the interactive experience.

**Actuation.** To enable wearable devices with output and feedback functions, researchers have explored methods to integrate various actuation mechanisms into fabrics to achieve deformation, vibration, or thermal responses. Shape memory alloy (SMA) actuators can produce controllable deformation under heating. For example, SMA-powered soft exosuits [42] can be used to assist individuals with limited mobility. Terrile et al. [39] proposed a tactile glove driven by SMA, which generates feedback by contracting and applying tension or resistance to the fingers when powered on. Electroactive polymers (EAP) [3] and dielectric elastomers [30, 52] deform under electric field control, simulating muscle-like movements or providing flexible actuation. Pneumatic actuators operate based on the compression and release of air to generate motion [27, 32, 34, 37]. Electromagnetic actuators [10, 14, 20, 26], leverage the interaction between magnetized materials and electromagnets to produce mechanical force and motions. They have been applied in a wide range of systems, including soft exoskeleton gloves for hand rehabilitation, soft robots capable of moving forward and backward, and interactive haptic interfaces that deliver tactile feedback in virtual reality.

Our system employs deformable magnetoactive materials in a compact design that eliminates the need for bulky, rigid frames or high-voltage drive modules. The actuation unit shares a unified structure with the sensing component and is seamlessly embedded within the fabric, preserving the system's softness, flexibility, and wearability.

## 2.2 Bidirectional Interactive Systems

Based on the research of sensing and feedback interfaces, researchers have begun to explore multifunctional wearable interfaces, aiming to achieve more complete and natural closed-loop interaction [16, 27, 37, 54]. For example, textile sensing gloves [26] with

tactile feedback units allow users to receive real-time vibration or pressure feedback directly while making gesture inputs. Others have also developed a textile interface [5] that combines capacitive touch sensing and display functions, achieving a combination of two-dimensional input and visual guidance or feedback. The system that integrates temperature sensing and controllable feedback [9] also shows promising prospects in health monitoring applications. However, currently most bidirectional interactive systems still rely on independent electronic modules [22] and are difficult to fully embed into textile structures. From the perspective of system integration, the sensing and actuation units are usually physically separated in these solutions, resulting in a large and complex structure that is difficult to meet the requirements of wearable applications for lightness, softness, and fit.

Our work has achieved an integrated design of sensing and actuation at the fabric level. The unified structure not only ensures excellent wearability, but also significantly enhances the compactness and consistency of the system, laying the foundation for a more immersive, seamless, and practical wearable interactive experience.

### 3 System Overview

MagTex consists of magnetoactive fibers and machine-knitted electromagnets. It leverages two complementary physical principles: the galvanomagnetic effect [51] and electromagnetic induction [41]. The galvanomagnetic effect enables the generation of alternating magnetic fields by passing the alternating current (AC) through the electromagnet, producing electromagnetic forces capable of actuating nearby magnetoactive materials (Fig. 2A). In MagTex, the AC-driven machine-knitted electromagnet produces an alternating electromagnetic field that interacts with magnetoactive fiber to induce vibrations at tunable frequencies and amplitudes (Fig. 2D and E). Conversely, electromagnetic induction generates the electromotive force (EMF) within the electromagnet in response to motion-induced variations in the local magnetic field, allowing the system to detect the relative movement of surrounding magnetoactive components (Fig. 2B). In MagTex, the motion of the magnetoactive fiber over the machine-knitted electromagnet induces a current via electromagnetic induction, enabling sensing and energy generation (Fig. 2F and G).

Through digital fabrication techniques, including fiber extrusion and digital knitting, MagTex achieves a scalable, spatially distributed interface that conforms to the body and integrates seamlessly into everyday garments. It offers comfort, adaptability, and the potential for human-centric interaction. The textile interface is designed to be worn like conventional garments, such as sleeves. We will detail the fabrication methodologies of MagTex and its integration into everyday textiles, demonstrating its potential for spatial, immersive, and adaptive interactive systems.

#### 3.1 Magnetoactive Fiber

The magnetoactive fiber is fabricated by extruding the magnetoactive ink composed of magnetic microparticles dispersed in the silicone elastomer matrix. To prepare the magnetoactive ink, the NdFeB microparticles (average diameter of 5  $\mu\text{m}$ , MQFP-B-20441-089, Magnequench) are mixed with the silicone elastomer matrix (Ecoflex 00-10, Smooth-On) at a weight concentration of 75 wt%

using a planetary mixer (DAC 330-100 PRO, FlackTek) operating at 3000 rpm for 1 minute. The resulting ink is immediately loaded into a dispensing syringe equipped with a single-channel needle and mounted onto a custom 3D printing system (System 30M, Hyrel 3D).

As illustrated in Fig. 3A, the magnetoactive ink is extruded through a tube and subsequently cured at room temperature for 12 hours. To fabricate fibers of different diameters, we utilize two sets of needle-tubing combinations with inner diameters of 2 mm and 1 mm, fabricating corresponding magnetoactive fibers. Due to the absence of magnetic alignment, the particles exhibit a random magnetic orientation at the fiber scale, as shown in Fig. 3B.

After curing and demolding, each fiber is folded at its midpoint and exposes to a pulsed magnetic field along its axial direction using an impulse magnetizer (IM-10-30, ASC Scientific), as depicted in Fig. 3B. After magnetization, the fiber is unfolded to restore its original shape. The resulting magnetic field distribution, shown on the right of Fig. 3B, reveals that the two ends of the fiber show the same polarity, while the center exhibits the opposite polarity, enabling bidirectional magnetic interaction across the fiber length. The magnetization pattern is programmable and can be tailored based on specific design requirements [53]. To achieve uniform control over the center region of the fiber for vibration under an alternating electromagnetic field, this magnetization approach is selected.

#### 3.2 Machine-knitted Electromagnet

The wearable machine-knitted electromagnet is achieved through the unique course-by-course, loop-over-loop machine knitting structure. It is fabricated using a 7-gauge computerized flatbed knitting machine (SWG091N2, Shima Seiki), as shown in Fig. 4. In this process, the yarn carrier moves horizontally to feed yarn into vertically actuated needles that are controlled by the carriage. As the carriage raises a needle, its slider opens, allowing yarn to be inserted. When the needle is lowered, the slider closes, pulling the new yarn through the loop from the previous course, thereby forming a loop-over-loop structure. After one cycle of carriage movement (from left to right and then back to the left), two courses of loops are formed, one in the left-to-right direction and another in the right-to-left direction (Fig. 5). Through this sequential process, knitted loops are formed course by course with the opposite direction. When knitting with magnet wire (34 AWG silver-plated copper wire with polyvinylidene fluoride insulation), the wires in adjacent courses run in opposite directions, enabling current flow in alternating directions. An electromagnet with a machine-knitted coil is formed at each interlock region (orange arrows in Fig. 5). A machine-knitted electromagnet patch consists of multiple coils distributed across a surface area.

To enhance mechanical integrity and dimensional stability, we also knit a base yarn (2/14 acrylic yarn, Tamm) to create supporting regions within the textile structure. The base yarn assists in shaping the magnet wire into uniform loops while knitting, contributing to the consistency of the knitted electromagnet. Additionally, the use of base yarn allows MagTex to be selectively integrated only in regions where sensing or haptic feedback is required. In areas

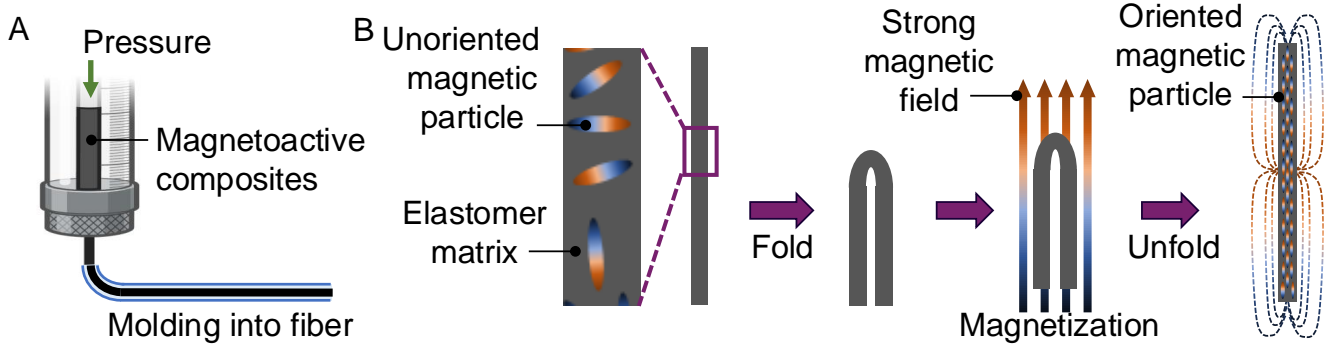


Figure 3: Magnetoactive fiber fabrication. A, Extrusion and B, Magnetization of magnetoactive fiber.

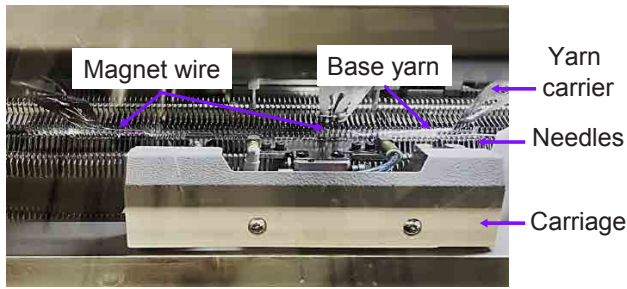


Figure 4: Digital machine knitting of electromagnet.

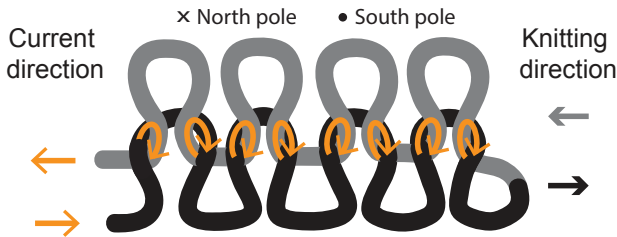


Figure 5: Distribution of machine-knitted electromagnets on a single-layer plain knit structure.

outside the interactive zones, the base yarn can be knitted as a normal garment, enabling seamless integration into everyday clothing while maintaining comfort and flexibility.

### 3.3 Sensing and Haptic Feedback Circuits

We design circuits for sensing signal acquisition and haptics control through a microcontroller board (ESP-WROOM-32 development board).

As shown in Fig. 6C, a sensing circuit is designed to amplify and condition the signal for downstream processing. Due to the extremely small induced EMF generated by the relative motion between the machine-knitted electromagnet and the magnetoactive fiber, which is typically in the microvolt ( $\mu$ V) range, the circuit employs a high-gain design (Gain = 99,381) to amplify the signal to a level that could be sampled by the internal analog-to-digital converter (ADC) of the microcontroller (MCU). The sensing circuit

includes two amplification stages, a voltage reference, and an offset adder, with filters and buffers between stages to reduce noise and maintain signal integrity. We use an AD8421 for differential first-stage amplification to suppress common-mode noise, followed by an OPA192 in a non-inverting second stage. Another OPA192 adds a DC offset from a precise voltage reference (ISL21010), ensuring the final signal fits the MCU's 0–3V ADC range. The MCU transmits 8-bit real-time data to a computer and receives corresponding feedback signals over Wi-Fi (Fig. 6D and E).

Our circuit generates 1 A AC to drive the haptics. We design a haptic feedback circuit (Fig. 6B) that outputs a square-wave AC with adjustable frequency and amplitude to drive the machine-knitted electromagnet. The circuit includes a constant voltage/constant current (CV/CC) module (XL4015 buck converter) and an H-bridge (DRV8833 motor driver). It operates in CV mode (5 V) until the output current reaches the preset limit, then switches to CC mode to maintain 1 A. This ensures CC through each coil. The MCU uses PWM to maintain a 100% output duty cycle in our design and utilizes GPIOs to set the output direction. The frequency of the generated square-wave AC is determined by the output switching rate.

To enable mode switching between sensing and haptic feedback functions in MagTex, a compact low-signal relay (G6A-274P-STUS) is applied to selectively connect MagTex to either the sensing circuit input or the haptic feedback circuit output (Fig. 6A). The relay is controlled by an external N-channel MOSFET (IRLML6344TRPBF, Infineon) in conjunction with the MCU's GPIO. A Schottky diode (BAT54) is connected in reverse parallel across the MagTex located in the relay's control section to suppress the high-voltage back EMF generated when the power is cut off, thereby protecting the MOSFET from breakdown.

The system is powered by two 3.7 V portable Li-ion batteries connected in series (totaling 7.4 V, 2600 mAh). We use a low dropout regulator (LT3045) to generate a stable 5 V voltage to drive the MCU and the haptic feedback circuit. Due to the bipolar nature of the induced EMF that the sensing amplification circuit needs to handle, we use a charge pump voltage converter (LT1054) to generate a negative voltage, forming a dual-rail power supply for the sensing circuit.

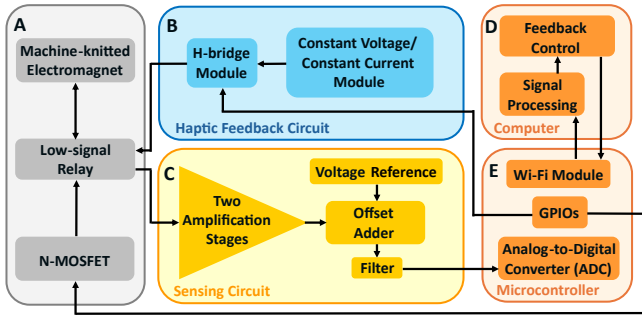


**Figure 6:** Circuit for sensing and haptic control. A, The MCU-controlled low-signal relay, driven by an N-MOSFET, switches the electromagnet between sensing and haptic feedback modes. B, The haptic feedback circuit uses a CV/CC module and an H-bridge to generate AC. C, The sensing circuit amplifies the EMF and shifts it into the MCU’s readable range. D, The computer receives real-time data via Wi-Fi and computes feedback signals. E, The MCU sends the sampled sensing data to the computer, and controls the haptic feedback circuit based on feedback.

### 3.4 Integration of MagTex

We develop three separate printed circuit boards (PCBs) for the power, sensing, and haptic feedback. Circuits are designed and stacked to form a three-layer structure (Fig. 7A and B). The MCU, H-bridge module, and batteries are assembled on the PCBs with a replaceable design, facilitating system maintenance. As depicted in Fig. 7C, to further protect the PCBs and make the system more portable, we 3D print a case that can fully enclose the stacked PCBs. The interior of the case has brackets that could hold the PCBs in place. The machine-knitted electromagnet and customized circuit are connected through standard JST XH connectors, which are easy to plug and unplug and have a stable connection. The case features openings on the front, back, and side to facilitate the insertion and removal of electromagnet and PCBs, and to enable convenient control of the power switches. In this way, the system inside the case only exposes the necessary ports through designated openings for connection with the external environment, enhancing simplicity, mobility, and deployability.

Upon completion of the magnetoactive fiber, machine-knitted electromagnet, and customized stacked PCBs, these components are integrated to form the MagTex system for bidirectional HMI. The magnetoactive fiber is manually sewn and fixed onto the machine-knitted electromagnet, achieving tight physical and functional coupling between the sensing and the haptic feedback components. The integrated system enables bidirectional interaction by sensing the motion of the magnetoactive fiber and driving current through the electromagnet, whose magnetic field interacts with the fiber to generate haptic output forces.

## 4 Result

This section presents characterization of the MagTex system, encompassing its material properties, sensing capabilities, and haptic performance. We evaluate the magnetic and mechanical behavior

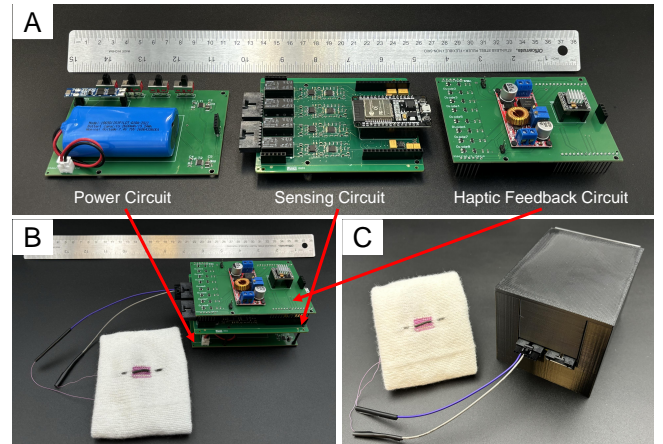


**Figure 7:** MagTex with integrated circuit. A, Customized PCBs for power, sensing, and haptic feedback circuit. B, MagTex textile connected to stacked PCBs for system operation. C, The system, enclosed in a protective case for stacked PCBs, features wireless connectivity, a compact design, and portability.

of both the magnetoactive fibers and the machine-knitted electromagnets. The sensing and haptic feedback functions are analyzed independently to identify optimal performance conditions for each modality. Thermal properties are also assessed to ensure the system’s safety for direct skin contact. Finally, user studies were conducted to evaluate practical usability and the perceptibility of haptic feedback. Collectively, these results provide a foundational understanding of MagTex’s performance and its potential for integration into wearable, bidirectional HMIs.

### 4.1 Characterization of Magnetoactive Fiber

The extruded magnetoactive fibers can be fabricated in two diameters: 2 mm and 1 mm, as shown in Fig. 8A. To evaluate their magnetic properties, fibers are magnetized under varying magnetic field strengths of 1.065, 1.424, 2.141, 2.836, 3.506, 4.149, and 4.733 T. The magnetic field generated by each fiber is measured using a Gaussmeter (GM2, AlphaLab), with the probe positioned at the midpoint of the fiber. Three specimens per fiber type are tested. Results indicate that increasing the magnetization field leads to a higher magnetic field strength in the fibers. As shown in Fig. 8B, both fiber types reach magnetic saturation at 2.141 T, beyond which additional increases in magnetization field strength produced negligible effects. The saturated magnetic flux density of the 2 mm fiber (45.9 mT) is approximately three times greater than that of the 1 mm fiber (14.9 mT), suggesting that the thicker fiber is more suitable for sensing applications where higher magnetic intensity is desired. However, the volume of the 2 mm fiber is approximately four times greater than that of the 1 mm fiber, which introduces potential magnetic losses due to the internal distribution of magnetic particles. Specifically, particles located nearer to the fiber core contribute less to the surface magnetic field, as their distance from the measurement point reduces their influence. Although the larger diameter allows the 2 mm fiber to achieve higher overall magnetic

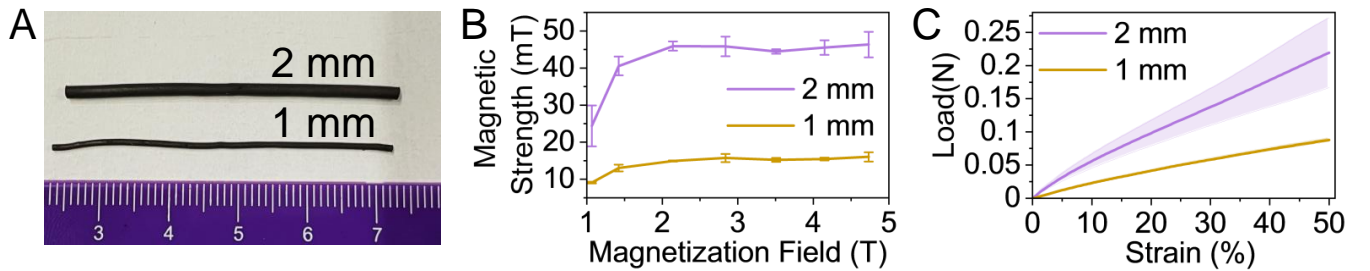


**Figure 8: Characterization of magnetoactive fiber.** A, Picture of extruded 2 and 1 mm magnetoactive fiber. B, The relationship between fiber magnetic strength and magnetization field strength. C, Tensile test of the magnetoactive fibers.

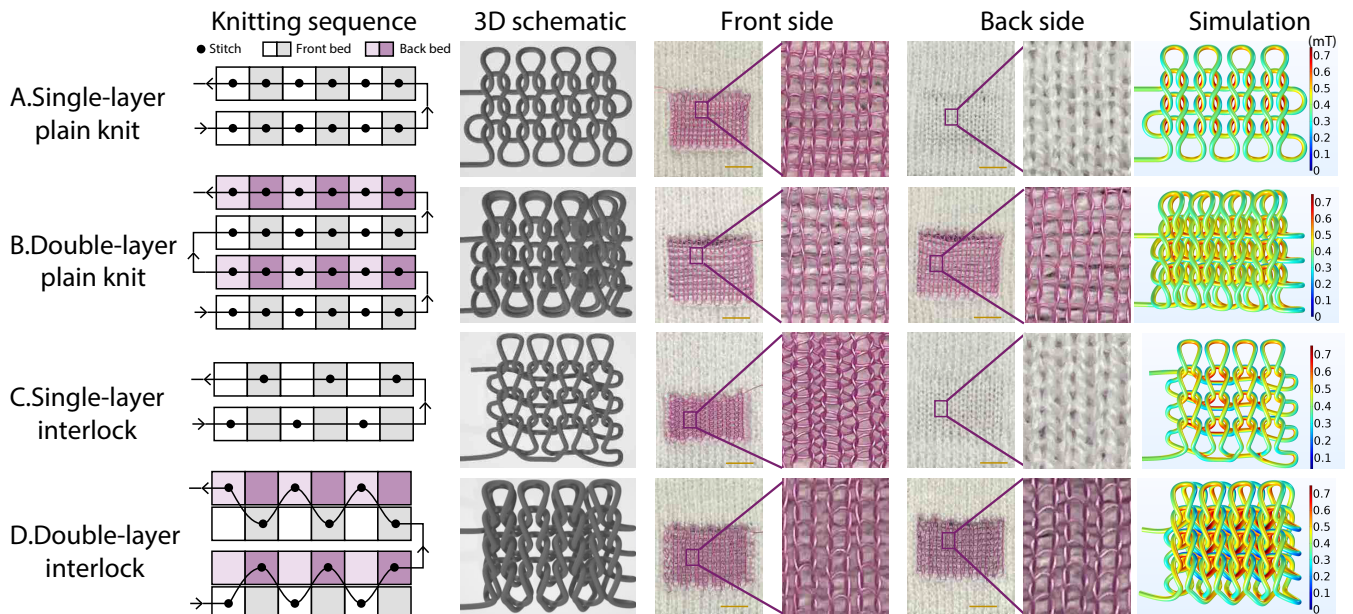


**Figure 9: Machine-knitted electromagnet structures.** Knitting sequence, 3D schematic, optical images, and simulated magnetic field distribution for: A, Single-layer plain knit. B, Double-layer plain knit. C, Single-layer interlock. D, Double-layer interlock.

strength, this volumetric effect can result in a reduced effective surface magnetic field. Since the surface field is critical for both sensing sensitivity and haptic feedback efficiency, such internal magnetic loss may limit the functional performance of thicker fibers in the haptic application.

Mechanical characterization is conducted on both fibers (2 mm and 1 mm diameter), each cut to a length of 200 mm. Tensile testing is performed using a universal testing machine (Instron 5585H) with a gauge length of 100 mm and a crosshead speed of 100 mm/min. The resulting load-strain curves are shown in Fig. 8C. The 2 mm fiber exhibits a breaking load of  $1.495 \pm 0.398$  N and a breaking strain of  $465.3\% \pm 77.0\%$ , while the 1 mm fiber showed a breaking load of  $0.420 \pm 0.049$  N and a breaking strain of  $401.7\% \pm 38.7\%$ . These results confirm the excellent stretchability of both fibers, making them well-suited for soft, wearable devices. Young's modulus, measured at 10% strain, is 1.8 kPa for the 2 mm fiber and 1.0 kPa for the 1 mm fiber. The lower stiffness of the thinner fiber makes it particularly

advantageous for haptic applications, where large deformations can be achieved under small magnetic forces.

## 4.2 Characterization of Machine-knitted Electromagnet

Four different knitting structures are designed for the fabrication of the machine-knitted electromagnets, as shown in Fig. 9A–D: single-layer plain knit, double-layer plain knit, single-layer interlock, and double-layer interlock. The single-layer plain knit is a fundamental weft knit structure produced on a single bed, consisting entirely of full loops. The double-layer plain knit is constructed on two beds, alternating plain-knit courses to form a two-layer fabric. The single-layer interlock structure is also knitted on a single bed, with loop patterns alternating along the needle bed. The double-layer interlock structure, formed on two beds, features alternating loops both along and across the needle bed.

In the single-layer plain knit and single-layer interlock structures, the magnet wire forming the machine-knitted electromagnets are exposed on the front side, while the base yarns fill the back side. In contrast, the double-layer plain knit and double-layer interlock structures exhibit symmetric configurations, with magnet wires and base yarns present on both sides of the fabric. As shown in the simulation results in Fig. 9, the flat machine-knitted electromagnet is strategically positioned at the interlocked region between adjacent loops, where the electromagnetic field strength is maximized.

Four machine-knitted electromagnet configurations are fabricated and systematically characterized to evaluate their performance. The goal is to identify an optimal design that maximizes both the galvanomagnetic effect for haptic feedback and electromagnetic induction for sensing. The electromagnetic field generated by the machine-knitted electromagnet is experimentally measured using a Gaussmeter, with input current ranging from 0.2 A to 2 A in 0.2 A increments. Corresponding theoretical electromagnetic field strengths are obtained through simulations based on machine-knitted electromagnet geometry and current input. As shown in Fig. 10, experimental values are represented by discrete data points, while the theoretical predictions are shown as continuous lines. The results demonstrate a linear relationship between the input current and the measured magnetic field strength, consistent with Ampère's right-hand grip rule, as expressed in Eq. 1.

$$B = \frac{\mu_0 NI}{2\pi r} \quad (1)$$

where  $B$  is the magnetic field strength,  $\mu_0$  is the permeability of free space,  $N$  is the number of turns,  $I$  is the current,  $r$  is the radius of the coil.

Among the tested structures, the interlock designs exhibited comparable magnetic field strength, due to their similar loop structures and current direction within a single conductive layer. Notably, the addition of a second layer in the double-layer structures does not result in enhanced magnetic field strength. This can be induced by the increased vertical separation between layers, which reduces the effective field contribution at the measurement point. The interlock structures generate magnetic fields approximately four times stronger than the single-layer plain knit. The plain knit structure demonstrated relatively weak field strength, likely due to opposing current directions in adjacent loops within the same wale, which leads to partial field cancellation. Based on these findings, the single-layer interlock structure is selected for subsequent applications as it produced the strongest electromagnetic field, an essential factor for effective haptic feedback.

The thermal behavior of the machine-knitted electromagnet with single-layer interlock is evaluated under cyclic power conditions at room temperature. A constant current of 1 A is applied in a pulsed manner—power on for 10 s followed by 10 s off. As shown in Fig. 11, the machine-knitted electromagnet temperature rises to 52.5 °C during the initial 10-second activation period and subsequently cools to 34.2 °C during the following 10-second rest phase. While the peak temperature exceeds human skin temperature (33–37 °C), the rapid cooling indicates efficient thermal dissipation. Furthermore, in practical applications, the machine-knitted electromagnet is not intended to be in direct contact with the skin, which mitigates

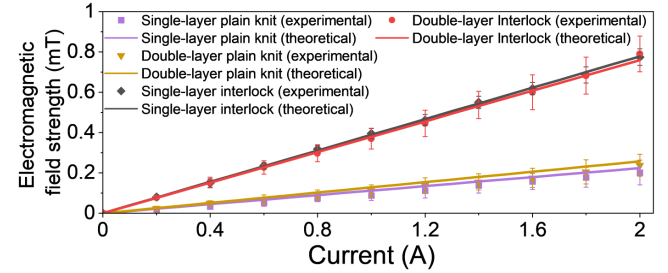


**Figure 10: Electromagnetic field strength of knitted electromagnet under different currents.**

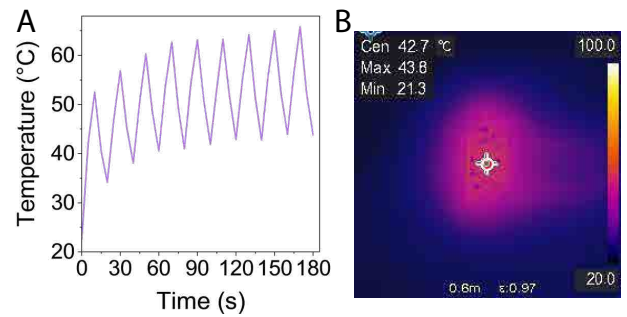


**Figure 11: Thermal characterization of single-layer interlock structure. A, Cyclic thermal test was conducted from 0 to 180 s. B, Thermal image captured at 180 s.**



**Figure 12: Bending test of knitted electromagnet.**

thermal safety concerns and supports its suitability for wearable use.

In addition to thermal performance, the machine-knitted electromagnet demonstrates excellent mechanical flexibility, as shown in Fig. 12. The machine-knitted electromagnet is bent along both the course and wale directions and returns to its original shape without any plastic deformation. This mechanical compliance shows the wearability of the machine-knitted electromagnet, making it well-suited for integration into soft, body-conforming wearable devices.

### 4.3 Sensing Characterization

To evaluate the sensing performance of the MagTex, two types of fiber motion—tapping and rolling—are tested. The tapping motion vertically presses the magnetoactive fiber by 5 mm toward the

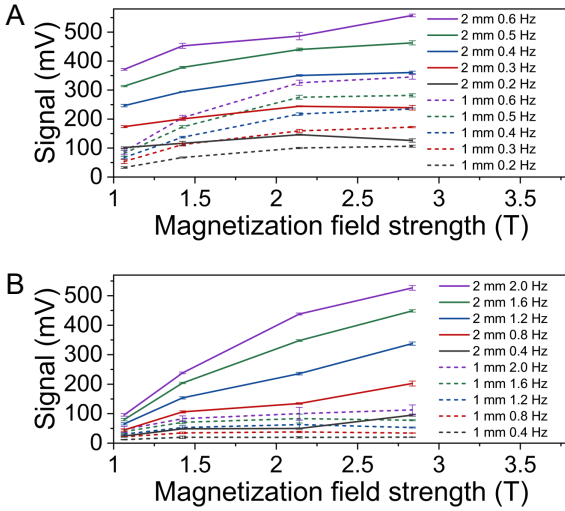


**Figure 13: Sensing function characterization of MagTex. A, Rolling motion test. B, Tapping motion test.**

knitted electromagnet, whereas the rolling motion horizontally rolls the magnetoactive fiber across the machine-knitted electromagnet surface with 20 mm displacement. We build a custom platform to evaluate sensors' response to the tapping and rolling motion, simulating realistic interactions. Tests were conducted at 0.2–2 Hz, matching the typical knee bending frequencies. The sensing signals are processed using a 4th-order Butterworth low-pass filter (50 Hz cutoff) in MATLAB. The amplified peak-to-peak voltages are calculated to show the sensing performance. Each test was repeated five times.

We test fibers of 1 mm and 2 mm in diameter with different magnetization strengths. According to Faraday's law of induction [12] (Eq. 2), the EMF induced in the machine-knitted electromagnet is directly proportional to the rate of magnetic flux change. Therefore, the frequency of tapping and rolling motions is varied to assess their effect on magnetic flux changes and resulting EMF.

As shown in Fig. 13, higher frequencies result in greater induced EMF in the knitted electromagnet, which aligns well with Faraday's law, as higher frequency magnetoactive movement indicates quicker magnetic flux change. Additionally, increasing the magnetization field strength of the fiber results in a higher induced EMF, as fibers with higher magnetic strengths generate greater magnetic flux changes prior to saturation. However, once the magnetization reaches saturation (around 2.141 T), further increases in magnetization strength do not significantly affect the induced EMF. In conclusion, the peak voltage increased with frequency and magnetic field strength, consistent with Equation 2.

$$\varepsilon = -N \frac{\Delta\Phi}{\Delta t} \quad (2)$$

where  $\varepsilon$  is the induced voltage,  $N$  is the number of loops (turns),  $\Delta\Phi$  is the change in magnetic flux, and  $\Delta t$  is the change in time.

To evaluate the sensing performance under mechanical deformation, we conducted tapping tests on a 20 × 30 mm knitted electromagnet subjected to bending at 0°, 30°, 60°, 90°, and 120° along both

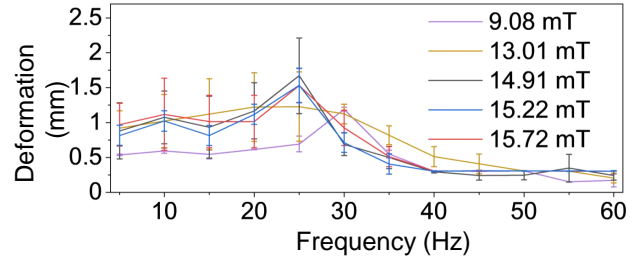


**Figure 14: Haptic function characterization. Deformation response of magnetoactive fibers with varying magnetic strengths (9.08, 13.01, 14.91, 15.22, and 15.72 mT) under actuation frequencies ranging from 5 to 60 Hz.**

the course and wale directions. The magnetoactive fiber was oriented along the wale direction. The amplitude of the signal remains consistent at  $330 \pm 40$  mV and  $350 \pm 30$  mV with bending along the course and wale directions, respectively. These demonstrate the stable and robust sensing capabilities of MagTex under various bending conditions.

#### 4.4 Haptics Characterization

The haptic function of the multifunctional MagTex is enabled by the actuation of magnetoactive fibers through the machine-knitted electromagnet. The deformation amplitude of the magnetoactive fiber during actuation serves as a key parameter for evaluating haptic performance, since the greater the actuation force induces the larger deformation of the magnetoactive fiber. In this study, 1 mm diameter magnetoactive fibers are integrated with the machine-knitted electromagnet consisting of 15 courses to investigate the effects of magnetic strength and actuation frequency on deformation behavior.

To examine the influence of magnetic strength, fibers are magnetized to flux densities of 9.08, 13.01, 14.91, 15.22, and 15.72 mT. Three specimens are tested for each magnetic strength. In addition to magnetic properties, haptic control frequency plays a critical role in performance, as the working principle of the system relies on vibrational motion induced by alternating electromagnetic fields. The samples are actuated using a 1 A AC power supply across a frequency range of 5 to 60 Hz in 5 Hz increments. The deformation amplitudes are captured using a digital camera (a7III, Sony), and the resulting displacements of the magnetoactive fiber were quantified through image analysis in ImageJ.

As shown in Fig. 14, the actuation deformation peaks in the range of 25–30 Hz. Prior to reaching this peak, deformation amplitude remains relatively stable across low frequencies, indicating that the magnetoactive fiber responds minimally at low frequencies. Within the 5–20 Hz range, fibers with higher magnetic strengths exhibit larger deformations due to increased magnetic forces. However, deformation gains plateau for fibers magnetized above 15 mT, due to magnetic saturation.

For the 9.08 mT fiber, the maximum deformation occurs at 30 Hz, while for fibers with higher magnetization, the peak shifts to 25 Hz. This shift might result from lower-magnetized fibers requiring higher frequency input to accumulate sufficient vibrational energy.

Once the magnetization exceeds approximately 13.01 mT, fibers consistently achieve peak deformation at 25 Hz. Beyond this frequency, deformation amplitude gradually decreases to a stable but lower level due to reduced deformation time per cycle at higher frequencies.

These findings provide insights for optimizing haptic performance in wearable systems. Magnetoactive fibers with magnetic strengths exceeding 15 mT, when actuated at 25 Hz, produced greater deformation amplitudes. However, higher actuation frequencies may also contribute to more significant haptic feedback, as they deliver higher energy per unit time to the skin. Further investigation is required to determine whether increased deformation or higher frequency vibrations result in more effective haptic perception. To this end, a user study is planned to explore this parameter space and identify the optimal actuation strategy for delivering perceivable haptic feedback.

#### 4.5 User Study on Haptic Feedback

As haptic feedback for users is highly subjective, we conducted a user study to evaluate the effectiveness of MagTex's haptic feedback performance across varying frequencies (20–60 Hz) and current amplitudes (0.2–1.2 A). The objective was to analyze how participants perceived tactile sensations, including intensity, contact area, vibration type, and temperature changes, while identifying trends in user responses across different parameter combinations.

**Participants.** Five participants ( $N = 5$ ; 3 males, 2 females), aged between 20 and 27 years ( $M = 22.17$ ,  $SD = 2.79$ ), were recruited for the study. All participants are right-handed and reported no prior hand injuries or conditions that could affect their tactile perception.

**Procedure.** The study began with a calibration session to familiarize participants with the actuator's feedback capabilities. During this session, participants were exposed to two extreme parameter combinations: the hypothesized strongest feedback (25 Hz at 1.2A) and the hypothesized weakest feedback (60 Hz at 0.2A). These calibration points were selected based on observed actuator behavior.

The main trials were conducted using a benchtop setup, where participants placed their right index finger lightly on the actuator fabric without deforming its surface or the underlying machine-knitted electromagnet structure (Fig. 15A). Visual indicators were provided to ensure consistent finger placement across trials, as shown in Fig. 15B. Each participant experienced 36 ten-second haptic feedback trials after the two pilot tests to establish scoring references. The participants experienced randomized combinations of six frequencies (20, 25, 30, 40, 50, and 60 Hz) and six currents (1.2, 1, 0.8, 0.6, 0.4, and 0.2 A). The blind testing protocol concealed parameter settings from participants to minimize bias in their responses. After each trial, participants provided feedback on perceived intensity using a scale from 0 to 10 and answered open-ended questions about their tactile experience. These questions prompted participants to describe the contact area (e.g., localized or spread), sensation type (e.g., weak, sharp, smooth), vibration characteristics (e.g., continuous, pulsing, buzzing), and any perceived temperature changes.

**Quantitative Results.** User response data collected from five participants were processed using Min-Max scaling, mapping intensity

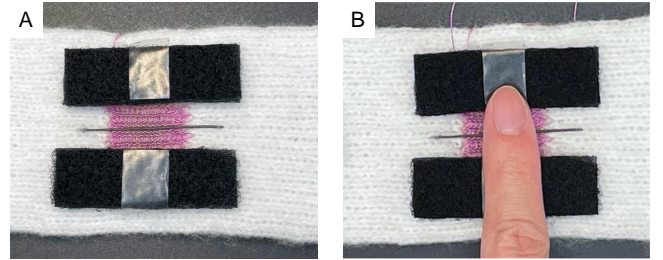


**Figure 15: Experimental setup for magnetoactive fiber user study.** A, Test configuration of the MagTex for the user study. B, Visual indicators used to guide finger placement during user interactions.

ratings onto a scale ranging from no sensation (0) to maximum sensation (10). Heatmaps, shown in Fig. 16, were generated for each participant to visually represent their perceived responses across all tested frequency-current combinations. Additionally, an aggregated heatmap, created by averaging individual responses, was generated to highlight general perceptual trends across participants. The use of a heatmap for this visualization is largely for the ease of parsing the graded user polarity in attitude for an otherwise two-dimensional dataset, as established in various fields of study [17, 18, 45].

The heatmaps revealed distinct patterns in how participants perceived the haptic feedback:

- **Higher Ratings for Lower Frequencies and Higher Currents:** Stronger sensations were observed at lower frequencies (20–40 Hz) combined with higher currents (0.8–1.2A). For example, the combination of 25 Hz at 1.2A consistently received high ratings across participants.
- **Lower Ratings for Higher Frequencies and Lower Currents:** Weaker sensations were reported at higher frequencies (50–60 Hz) paired with lower currents (0.2–0.6A). These combinations frequently received ratings of 0/10 or near-zero values.
- **Gradual Decrease in Ratings Across Parameters:** A general trend of decreasing ratings was observed as frequency increased or current decreased.

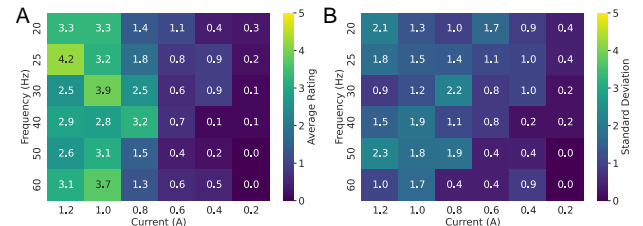


**Figure 16: User perception of MagTex haptic feedback intensity.** A, Average perceived intensity ratings aggregated across all participants. B, Variability in perceived intensity highlighting individual differences among participants.

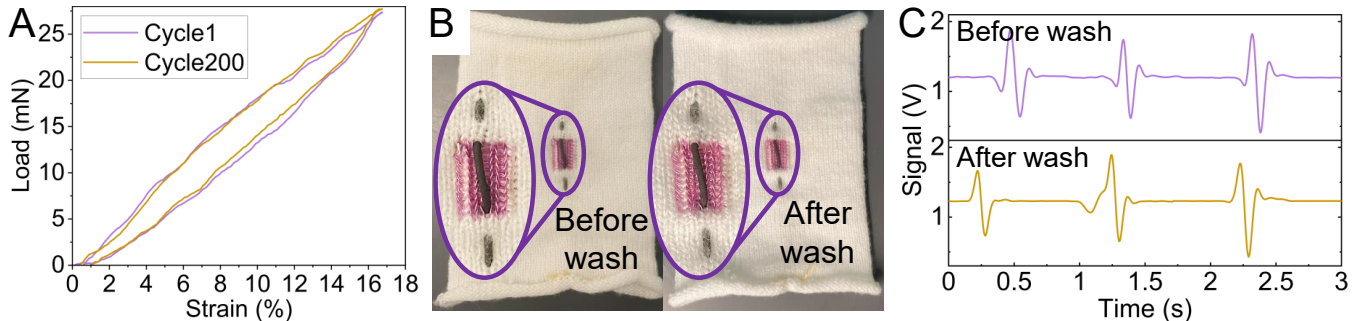


**Figure 17:** A, Cyclic tensile test for magnetoactive fiber. B, MagTex structure before wash (left) and after wash (right). C, Signal from tapping on MagTex before and after wash.

The aggregated heatmap in Fig. 16 further highlighted these trends, showing a concentration of higher ratings in the lower frequency-higher current quadrant and lower ratings elsewhere.

**Qualitative Results.** Participants provided detailed descriptions of their experiences with the haptic sensation from the MagTex. Participants frequently commented on vibration intensity and stability depending on the frequency-current combinations tested. Lower frequencies (20–30 Hz) elicited descriptions like “scratchy tapping” or “discontinuous pulses,” while higher frequencies (40–60 Hz) were described as “phone-like buzzing” or “stable vibrations.” Temperature changes were inconsistently reported; only two participants noted perceiving heat during higher-current trials as “gradual” or “slight.” Contact area descriptions varied widely with terms like “line,” “point,” or “square” recurring across responses. Feedback ranged from discomfort to enjoyment, depending on parameter combinations tested. Lower frequencies sometimes caused discomfort (“scratchy” or “itchy”), while mid-range parameters like 30 Hz at 1A were described as “gentle” or “soothing.” Ambiguity was common at lower currents, where some participants expressed uncertainty (“unsure if I felt anything”). Participants often used analogies to describe sensations: one participant likened low-frequency vibrations to “a fly flapping its wings,” while another described high-frequency vibrations as “a phone buzzing.”

The combined quantitative and qualitative findings revealed several important trends:

- **Parameter Impact:** Higher currents produced stronger sensations across all users; higher frequencies reduced perceptual clarity.
- **Individual Variability:** Callused skin reduced sensitivity; physiological differences influenced perception.
- **Design Implications:** Lower frequencies paired with higher currents are optimal for delivering distinct haptic feedback.

Overall, the study confirms that the magnetoactive fiber actuator can deliver diverse haptic feedback patterns effectively across varying parameters.

#### 4.6 Durability

As a textile-based HMI, long-term durability and washability are critical requirements for MagTex. We assess the long-term durability of magnetoactive fiber through evaluation on their magnetic

and mechanical properties. Magnetic strength is particularly critical, as it directly influences the magnitude of the magnetic force generated during haptic feedback. After four months of storage, the magnetoactive fibers retained their magnetic strength ( $14.92 \pm 0.83$  mT), showing no significant degradation compared to the initial value ( $15.22 \pm 0.54$  mT).

To evaluate the mechanical fatigue behavior of the magnetoactive fiber under haptic operation conditions, a 200-cycle tensile fatigue test was conducted at a loading speed of 50 mm/min and a maximum strain of 17%. As shown in Fig. 17A, the test resulted in only a 3.5% decrease in Young’s modulus, indicating minimal mechanical degradation.

To assess its washability, we wash MagTex for a 30-minute wash cycle using a commercially available washing machine (Magtag Washer). As shown in Fig. 17B, the structure of MagTex remains unchanged after washing. The magnetic strength of the magnetoactive fiber shows a slight decrease, from 17.04 mT to 15.84 mT. The sensing performance is preserved; in response to tapping stimuli, the after-wash signal amplitude ( $1.17 \pm 0.17$  V) remains comparable to the before-wash value ( $1.26 \pm 0.12$  V), with consistent signal waveforms (Fig. 17C).

## 5 Application

MagTex supports both independent sensing and haptic feedback functionalities, as well as fully integrated closed-loop operation, bidirectional interaction from sensing to haptic feedback. Three example applications are presented below to demonstrate their capabilities. A smart sleeve functions as a wireless soft controller for a video game, where the MagTex acts as a motion-responsive input device capable of real-time gesture recognition. A tactile Braille display glove illustrates the use of localized haptic feedback to encode and transmit Braille characters for visually impaired users. Additionally, a closed-loop system integrates a smart knee brace and glove, in which the textile simultaneously senses running speed and delivers real-time haptic feedback to guide user performance. Together, these applications demonstrate the potential of the MagTex to seamlessly combine sensing and haptic feedback in a soft, scalable, and large spatial coverage format.

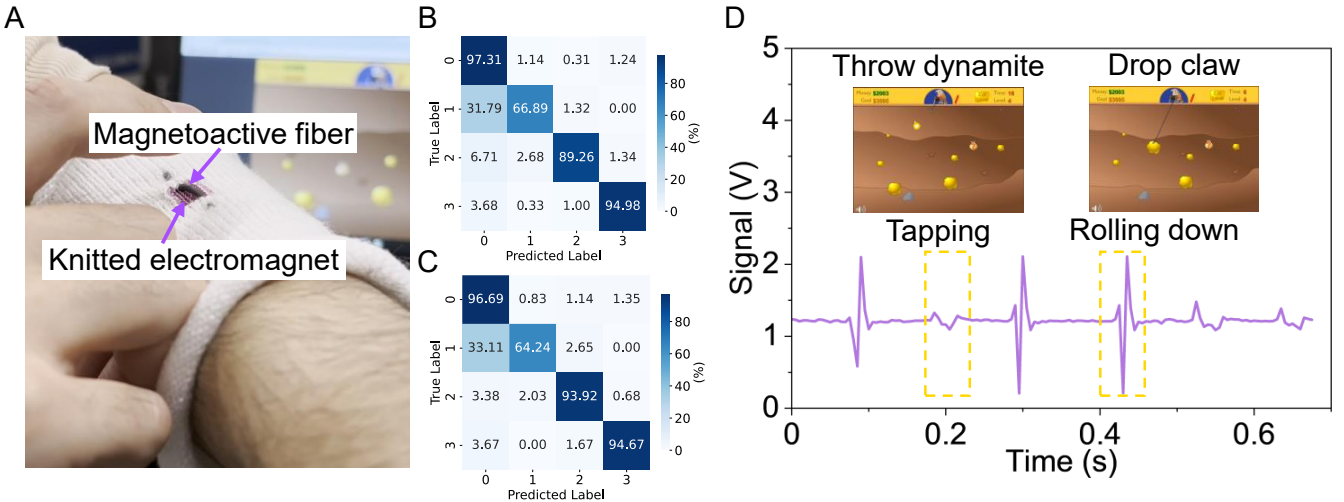


**Figure 18: Wearable controller utilizing MagTex for video game interaction.** A, MagTex integrated into a smart sleeve as a game controller. Confusion matrix of the prediction results for training the Random Forest model on B, the original dataset and C, the extracted features. D, Real-time signals and predictions during the video game.

### 5.1 Wireless Game Controller Sleeve

The relative movement between the magnetoactive fiber and the machine-knitted electromagnet induces an electromotive force via electromagnetic induction, which can be detected and used as a sensing signal. To demonstrate this capability, we develop a wireless soft controller for video games. As shown in Fig. 18A, a smart sleeve is fabricated with a MagTex unit embedded at the forearm. A 2 mm-diameter magnetoactive fiber, magnetized at 4.733 T, is manually sewn onto the machine-knitted electromagnet, which is knitted using magnet wire in a single-layer plain knit pattern consisting of 10 courses and 6 wales.

The smart sleeve is connected to a customized circuit equipped with Wi-Fi functionality, enabling wireless communication with a computer. This configuration allows the sleeve to operate as a standalone wireless controller. The magnetoactive fiber responds to mechanical interactions—such as tapping or rolling—which generate distinct signal patterns.

To demonstrate the interaction ability as an input controller of the smart sleeve, four fiber motion states are defined and tested: static (0), tapping (1), rolling up (2), and rolling down (3). We employ a random forest classifier for real-time motion recognition. Feature extraction uses eight signal features: mean, standard deviation, minimum value, maximum value, energy, voltage peak-to-peak, dominant frequency, entropy, and harmonic ratio. We compute these features using a sliding-window approach with a window size of 80 samples and a step size of 10, based on the observation that a single waveform contains approximately 70 data points with a 200 Hz sampling rate. In total, 7,824 data points are collected to train and evaluate the random forest (RF) model. Of these, 5,007 (64%) data points are used for training, 1,252 (16%) for validation, and the remaining 1,565 (20%) for testing the model's performance.

We evaluate the classifier trained on both the raw signal data and the extracted feature set. The model trained on raw data achieves

an accuracy of 93.10%, while the model trained on the extracted features reaches 92.91%. This indicates that the selected features capture most of the critical information within the dataset.

The classification results are shown in Fig. 18B. The rolling motions (classes 2 and 3) and static state (class 0) are predicted with high accuracy. However, the tapping motion (class 1), characterized by a relatively low signal amplitude, is occasionally misclassified as the static state approximately 30% of the time. This may be due to the weak signal amplitude generated by the tapping motion, resulting in signal features that closely resemble background noise and are more easily misclassified as the static state.

As shown in Fig. 18A, the fabricated smart sleeve can be directly worn on the forearm, functioning as a wireless controller. Two specific gestures are implemented for gameplay interaction, as shown in Fig. 18D with real-time signal classification. Rolling the magnetoactive fiber downward triggers the "down" key event, releasing the hook to capture gold. Tapping the fiber triggers the "up" key event, which releases a bomb when an undesired object (e.g., a stone) is captured. Compared to the default keyboard input for the game, the smart sleeve provides a more intuitive interaction—rolling down to release the hook and tapping to detonate the bomb—enhancing user immersion and usability. The system exhibited fast response time without noticeable delay during gameplay, as demonstrated in the Supplementary movie.

### 5.2 Braille Display Glove

In addition to its sensing capability, the haptic function of the multifunctional MagTex is particularly well-suited for developing haptic feedback devices. We demonstrate this functionality through a tactile communication system designed for visually impaired individuals. Braille is a tactile reading and writing system that encodes characters using combinations of raised dots. The MagTex unit is ideal for representing these dots due to its localized vibrational feedback and soft, flexible form factor.

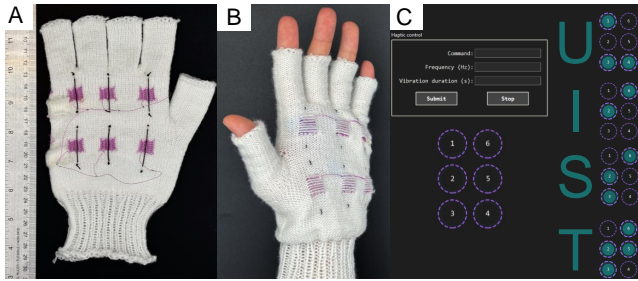


**Figure 19: MagTex for Braille display.** A, Smart glove with six integrated MagTex units. B, Glove worn by user, delivering Braille-based haptic feedback via palm-mounted units. C, Braille character layout with an example sequence displaying "UIST".

We develop a smart glove integrated with six MagTex units corresponding to the six-dot Braille cell, as shown in Fig. 19A. Each unit is composed of a 50 mm magnetoactive fiber, manually sewn onto the glove surface. The machine-knitted electromagnet for each unit is knitted directly into the glove using a single-layer interlock structure (7 courses  $\times$  4 wales) with magnet wire.

During operation, the MagTex units are actuated at 25 Hz using 1 A AC power to simulate the sensation of a raised Braille dot. This behavior is illustrated in the movie (Supplementary Materials). A custom user interface is developed to facilitate real-time Braille character display, as shown in Fig. 19B. Users can input characters via a text field labeled "Command". Upon clicking the submit button, the corresponding magnetoactive units activate and vibrate to form the Braille representation of the selected character. For example, inputting "U" and clicking submit activates units 1, 3, and 4, which correspond to the Braille encoding of that character.

As shown in Fig. 19C, the smart glove can be worn like a normal glove, with the Braille display positioned on the palm. This configuration enables users to perceive character feedback through tactile vibrations at their palms, offering a wearable and intuitive solution for non-visual communication.

### 5.3 Closed-loop Running Speed Monitor

The multifunctional MagTex integrates both sensing and haptic functionalities, enabling closed-loop interaction without the need for external sensors or feedback interference. To demonstrate this capability, we develop a smart knee brace in combination with a smart glove, forming a fully integrated closed-loop system.

As illustrated in Fig. 20, a MagTex unit is embedded at the middle of the knee brace to monitor leg bending speed. For this application, a 2 mm-diameter magnetoactive fiber, magnetized at 4.733 T, is used to ensure sufficient magnetic responsiveness. The machine-knitted electromagnet is fabricated using magnet wire knitted into a single-jersey jacquard structure consisting of 10 courses and 6 wales. The magnetoactive fiber is then manually sewn onto the surface of the coil to complete the textile-based sensing unit.

The smart knee brace integrates MagTex at the knee joint to monitor motion and provides haptic feedback via an actuator positioned on the dorsal side of the right hand (Fig. 20A). This location

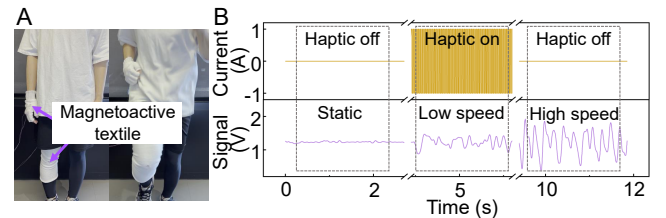


**Figure 20: Closed-loop system for running speed monitoring and real-time haptic feedback.** A, MagTex integrated into a smart knee brace and glove for sensing and haptic feedback. B, Real-time monitoring signal indicating running speed (bottom) and corresponding haptic feedback control output current delivered to the glove (top).

was selected for its stability during movement and high tactile sensitivity, ensuring consistent and effective feedback delivery.

This system detects different motion speeds based on the signal amplitude generated by the magnetoactive fiber: slower movements produce lower amplitude signals, while faster motions result in higher signal amplitudes, as shown in the lower part of Fig. 20B. For haptic feedback, one of the MagTex units is integrated onto the back of the hand within the smart glove. This placement minimizes interference from finger movement, especially since the hand is typically in a fist posture during running.

The knee brace continuously monitors running activity. As illustrated in Fig. 20B, when the user is stationary (speed = 0), no haptic feedback is triggered, as running has not yet begun. During low-speed running, the glove's haptic unit is activated using a square-wave AC signal (1 A, 25 Hz), delivering a tactile warning to encourage increased speed. Once the desired speed threshold is reached, the haptic feedback is deactivated, indicating successful performance (see Supplementary movie).

This application highlights the potential of multifunctional MagTex for closed-loop systems in sports and motion capture scenarios, offering a compact, soft, and self-contained platform for real-time sensing and feedback.

## 6 Discussion

The multifunctional MagTex presented in this work offers an integrated platform for both sensing and haptic feedback, enabling bidirectional interaction in a soft and wearable form. This design addresses the long-standing challenge in smart textiles of achieving co-located and seamless integration of multiple functionalities while maintaining comfort, flexibility, and scalability. Although the system demonstrates promising results, certain technical limitations must be addressed to fully realize its scalability and performance in real-world applications.

*Magnetoactive fiber extrusion.* The current fiber fabrication process relies on thermal-curing materials, which require long curing times and do not allow instant solidification after extrusion. This thermal requirement, combined with a tubing-based extrusion method, imposes constraints on production scalability and limits flexibility in customizing fiber dimensions. Furthermore, the extrusion-molding approach inherently limits the fiber length due to the high extrusion pressure required within the tubing during

fabrication. To address these limitations, future directions include developing UV-curable magnetoactive inks to enable continuous fiber production. Unlike thermal-curing materials, UV-curable materials offer rapid, on-demand curing and eliminate constraints on fiber length [36, 49].

*Mechanical structure design of MagTex.* Another challenge is the mechanical instability of the system during dynamic use, which may affect haptic feedback consistency. Misalignment of the magnetoactive fiber can lead to inconsistent actuation, reducing the reliability of haptic feedback. This occurs when the fiber shifts away from the desired position within the electromagnetic field during activation, resulting in reduced or uneven vibrational output. This highlights the need for improved mechanical integration strategies to ensure consistent fiber positioning and performance. Further work will focus on optimizing the design and alignment of machine-knitted electromagnets and magnetoactive fibers to ensure consistent and reliable actuation. Additionally, exploring advanced integration strategies such as improved textile architectures and encapsulation techniques will be essential to enhance the robustness and stability of haptic feedback under dynamic, real-world conditions.

*Circuitry.* In terms of circuits, the current system uses low-signal relays to switch between sensing and haptic feedback modes for machine-knitted electromagnets. Although relays are suitable for driving haptics with AC, their mechanical structure presents challenges such as bulky size, limited lifespan, and additional power consumption when energized, limiting further circuit integration. There are circuit-level improvements, such as adopting bidirectional conducting MOSFET arrays or analog switches to enable compact, fast, and energy-efficient mode switching.

*Application.* Importantly, the demonstrated applications highlight the platform's versatility across interaction examples. The wireless game controller illustrates the potential for intuitive gesture-based input, the Braille glove exhibits localized haptic feedback for accessibility, and the combination of the smart knee brace and glove shows real-time sensing-haptic feedback in a closed-loop system. These examples underline the potential of this technology to impact assistive devices, wearable controllers, and immersive environments.

## 7 Conclusion

In this work, we present MagTex, a machine-knitted magnetoactive textile that integrates both sensing and haptic feedback capabilities into a unified wearable platform. By combining custom-extruded magnetoactive fibers with digitally knitted electromagnets, MagTex enables bidirectional HMI through two fundamental physical mechanisms: the galvanomagnetic effect for haptic feedback and electromagnetic induction for sensing. Our design addresses key challenges in smart textile systems, including spatial coverage, wearability, and seamless integration of multimodal functionality. We demonstrate the feasibility and versatility of MagTex through systematic material characterization, device performance evaluation, user studies, and application prototypes, including a wireless soft game controller, a wearable Braille display glove, and a closed-loop knee brace system that provides real-time running speed feedback. The system shows promising performance in terms of magnetic

responsiveness, mechanical durability, and user-perceived haptic feedback. This work demonstrates a fabric-level bidirectional HMI that is soft and compatible with the scalable textile manufacturing approaches. Future research will focus on improving fabrication efficiency, enhancing haptic feedback stability, and expanding multimodal feedback for broader deployment in assistive technology, immersive interfaces, and next-generation wearables.

## Acknowledgments

We acknowledge support from the Royalty Research Fund at the University of Washington.

## References

- [1] Beyza Bozali, Sepideh Ghodrat, and Kaspar M. B. Jansen. 2023. Design of Wearable Finger Sensors for Rehabilitation Applications. *Micromachines* 14, 4 (2023). <https://doi.org/10.3390/mi14040710>
- [2] Lorenzo Capineri. 2014. Resistive sensors with smart textiles for wearable technology: from fabrication processes to integration with electronics. *Procedia Engineering* 87 (2014), 724–727.
- [3] Yue Chen, Fujian Zhang, Guanggui Cheng, Jian Jiao, and Zhongqiang Zhang. 2025. Advances in electroactive polymer-based haptic actuators for human-machine interfaces: from principles to applications. *Advanced Manufacturing* 2, 1 (2025), 0004. <https://doi.org/10.55092/am20250004>
- [4] Aonan Cheng, Xiaoyuan Li, Dongdong Li, Wenkai Zhang, Meng Zhang, Qiang Zeng, Tao Liu, Zhen Wang, Runwei Li, Litao Liu, Zhenxing Wang, Zhi Zhang, and Xiaonan Wang. 2025. An intelligent hybrid-fabric wristband system enabled by thermal encapsulation for ergonomic human-machine interaction. *Nature Communications* 16 (2025), 591. <https://doi.org/10.1038/s41467-024-55649-1>
- [5] Hyung Woo Choi, Dong-Wook Shin, Jiajie Yang, Sanghyo Lee, Cátia Figueiredo, Stefano Sinopoli, Kay Ullrich, Petar Jovančić, Alessio Marrani, Roberto Momentè, João Gomes, Rita Branquinho, Umberto Emanuele, Hanleem Lee, Kwang-Ho Cho, Jae-Hoon Kim, Jae-Hong Kim, Seung-Beck Lee, Seung-Hwan Lee, and Young-Jin Kim. 2022. Smart textile lighting/display system with multifunctional fibre devices for large scale smart home and IoT applications. *Nature Communications* 13 (2022), 814. <https://doi.org/10.1038/s41467-022-28459-6>
- [6] Viktorija Diak and Andrii Diak. 2025. Smart textile as advanced human digital interface in metaverse. *The Design Journal* (2025), 1–27.
- [7] Kai Dong, Xiao Peng, Jie An, Aurelia Chi Wang, Jianjun Luo, Baozhong Sun, Jie Wang, and Zhong Lin Wang. 2020. Shape adaptable and highly resilient 3D braided triboelectric nanogenerators as e-textiles for power and sensing. *Nature communications* 11, 1 (2020), 2868.
- [8] Xing Fan, Jun Chen, Jin Yang, Peng Bai, Zhaoling Li, and Zhong Lin Wang. 2015. Ultrathin, rollable, paper-based triboelectric nanogenerator for acoustic energy harvesting and self-powered sound recording. *ACS nano* 9, 4 (2015), 4236–4243.
- [9] Zixiao Feng, Heqing Ye, Yufei Lu, Hongjian Zhang, Zhenguo Liu, and Wei Huang. 2025. Flexible intelligent thermal management systems: Sensing devices, signals, and applications. *Nano Energy* 138 (2025), 110842. <https://doi.org/10.1016/j.nanoen.2025.110842>
- [10] Matthew T Flavin, Kyoung-Ho Ha, Zengrong Guo, Shupeng Li, Jin-Tae Kim, Tara Saxena, Dimitrios Simatos, Fatimah Al-Najjar, Yuxuan Mao, Shishir Bandapalli, et al. 2024. Bielastic state recovery for haptic sensory substitution. *Nature* (2024), 1–8.
- [11] Daniel Geißler, Bo Zhou, Hymalai Bello, Joanna Sorysz, Lala Ray, Hamraz Javaheri, Matthias Rüb, Jan Herbst, Esther Zahn, Emil Woop, et al. 2024. Embedding textile capacitive sensing into smart wearables as a versatile solution for human motion capturing. *Scientific Reports* 14, 1 (2024), 15797.
- [12] Nathan Ida and Nathan Ida. 2015. Faraday's law and induction. *Engineering Electromagnetics* (2015), 515–563.
- [13] Hyungseok Kang, Chunlin Zhao, Jinrong Huang, Dong Hae Ho, Yonas Tsegaye Megra, Ji Won Suk, Jia Sun, Zhong Lin Wang, Qijun Sun, and Jeong Ho Cho. 2019. Fingerprint-inspired conducting hierarchical wrinkles for energy-harvesting e-skin. *Advanced Functional Materials* 29, 43 (2019), 1903580.
- [14] Nikolas Kastor, Bharat Dandu, Vedad Bassari, Gregory Reardon, and Yon Visell. 2023. Ferrofluid electromagnetic actuators for high-fidelity haptic feedback. *Sensors and Actuators A: Physical* 355 (2023), 114252. <https://doi.org/10.1016/j.sna.2023.114252>
- [15] Kyobin Keum, Jae Sang Heo, Jimi Eom, Keon Woo Lee, Sung Kyu Park, and Yong-Hoon Kim. 2021. Highly Sensitive Textile-Based Capacitive Pressure Sensors Using PVDF-HFP/Ionic Liquid Composite Films. *Sensors* 21, 2 (2021), 442. <https://doi.org/10.3390/s21020442>
- [16] Jonathan P King, Luis E Valle, Nishant Pol, and Yong-Lae Park. 2017. Design, modeling, and control of pneumatic artificial muscles with integrated soft sensing.

- In *2017 IEEE International Conference on Robotics and Automation (ICRA)*. IEEE, 4985–4990.
- [17] Paul Klemm, Kai Lawonn, Sylvia Glaßer, Uli Niemann, Katrin Hegenscheid, Henry Völzke, and Bernhard Preim. 2015. 3D regression heat map analysis of population study data. *IEEE transactions on visualization and computer graphics* 22, 1 (2015), 81–90.
- [18] Matthias Kraus, Katrin Angerbauer, Juri Buchmüller, Daniel Schweitzer, Daniel A Keim, Michael Sedlmair, and Johannes Fuchs. 2020. Assessing 2d and 3d heatmaps for comparative analysis: An empirical study. In *Proceedings of the 2020 CHI Conference on Human Factors in Computing Systems*. 1–14.
- [19] Seulah Lee, Yuna Choi, Minchang Sung, Jihyun Bae, and Youngjin Choi. 2021. A Knitted Sensing Glove for Human Hand Postures Pattern Recognition. *Sensors* 21, 4 (2021). <https://doi.org/10.3390/s21041364>
- [20] Dongdong Li, Jiawei He, Ziyang Song, Minghao Luo, Xu Zhao, Ziling Xue, Ying Li, Lianwan Jin, Chuanxin Yu, and Nanshu Lu. 2021. Miniaturization of mechanical actuators in skin-integrated electronics for haptic interfaces. *Microsystems & Nanoengineering* 7 (2021), 85. <https://doi.org/10.1038/s41378-021-00301-x>
- [21] Zhiming Lin, Zhiyi Wu, Binbin Zhang, Yi-Cheng Wang, Hengyu Guo, Guanlin Liu, Chaoyu Chen, Yuliang Chen, Jin Yang, and Zhong Lin Wang. 2019. A triboelectric nanogenerator-based smart insole for multifunctional gait monitoring. *Advanced Materials Technologies* 4, 2 (2019), 1800360.
- [22] Han Liu, Yihui Shi, Yihong Pan, Wei Zhang, Jiayi Wang, Zihan Wu, Fei Wang, Yunling Zhang, Hong Li, Lei Lin, Yan Zhu, Yong Huang, and Huisheng Peng. 2025. Sensitive interactive fibers and textiles. *npj Flexible Electronics* 9 (2025), 23. <https://doi.org/10.1038/s41528-025-00398-4>
- [23] Zheng Lou, Lili Wang, Kai Jiang, Zhongming Wei, and Guozhen Shen. 2020. Reviews of wearable healthcare systems: Materials, devices and system integration. *Materials Science and Engineering: R: Reports* 140 (2020), 100523.
- [24] Pasindu Lugoda, Edgar S. Oliveros-Mata, Kalana Marasinghe, Theo Hughes-Riley, Niko Münzenrieder, Denys Makarov, and Tilak Dias. 2025. Submersible touchless interactivity in conformable textiles enabled by highly selective overbraided magnetoresistive sensors. *Communications Engineering* 4 (2025), 33. <https://doi.org/10.1038/s44172-025-00373-x>
- [25] Yiyue Luo, Yunzhu Li, Michael Foshey, Wan Shou, Pratyusha Sharma, Tomás Palacios, Antonio Torralba, and Wojciech Matusik. 2021. Intelligent carpet: Inferring 3d human pose from tactile signals. In *Proceedings of the IEEE/CVF conference on computer vision and pattern recognition*. 11255–11265.
- [26] Yiyue Luo, Chao Liu, Young Joong Lee, Joseph DelPreto, Kui Wu, Michael Foshey, Daniela Rus, Tomás Palacios, Yunzhu Li, Antonio Torralba, et al. 2024. Adaptive tactile interaction transfer via digitally embroidered smart gloves. *Nature communications* 15, 1 (2024), 868. <https://doi.org/10.1038/s41467-024-45059-8>
- [27] Yiyue Luo, Kui Wu, Andrew Spielberg, Michael Foshey, Daniela Rus, Tomás Palacios, and Wojciech Matusik. 2022. Digital Fabrication of Pneumatic Actuators with Integrated Sensing by Machine Knitting. In *Proceedings of the 2022 CHI Conference on Human Factors in Computing Systems* (New Orleans, LA, USA) (CHI '22). Association for Computing Machinery, New York, NY, USA, Article 175, 13 pages. <https://doi.org/10.1145/3491102.3517577>
- [28] Yiyue Luo, Junyi Zhu, Kui Wu, Cedric Honnet, Stefanie Mueller, and Wojciech Matusik. 2023. MagKnitc: Machine-knitted Passive and Interactive Haptic Textiles with Integrated Binary Sensing. In *Proceedings of the 36th Annual ACM Symposium on User Interface Software and Technology* (San Francisco, CA, USA) (UIST '23). Association for Computing Machinery, New York, NY, USA, Article 66, 13 pages. <https://doi.org/10.1145/3586183.3606765>
- [29] Sara S. Mechael, Yunyun Wu, Yiting Chen, and Tricia Breen Carmichael. 2021. Ready-to-wear strain sensing gloves for human motion sensing. *iScience* 24, 6 (2021), 102525. <https://doi.org/10.1016/j.isci.2021.102525>
- [30] Johannes Mersch, Sascha Pfeil, Felix Lohse, Henriette Probst, Chokri Cherif, and Gerald Gerlach. 2019. Textile-Amplified Dielectric Elastomer Actuators for Soft Robotics. In *Proceedings of the 19th World Textile Conference AUTEX 2019: Textiles at the Crossroads*. Ghent University, Ghent, Belgium. <https://openjournals.ugent.be/autex/article/63824/galley/188198/view/>
- [31] Dimitris Mourtzis, John Angelopoulos, and Nikos Panopoulos. 2023. The future of the human–machine interface (HMI) in society 5.0. *Future Internet* 15, 5 (2023), 162.
- [32] Phuong H. Nguyen and Wei Zhang. 2020. Design and Computational Modeling of Fabric Soft Pneumatic Actuators for Wearable Assistive Devices. *Scientific Reports* 10 (2020), 9638. <https://doi.org/10.1038/s41598-020-65003-2>
- [33] Lili Pan, Yali Xie, Hualin Yang, Mengchao Li, Xilai Bao, Jie Shang, and Run-Wei Li. 2023. Flexible Magnetic Sensors. *Sensors* 23, 8 (2023), 4083. <https://doi.org/10.3390/s23084083>
- [34] Jiaming Qi, Feng Gao, Guanghui Sun, Joo Chuan Yeo, and Chwee Teck Lim. 2023. HaptGlove—untethered pneumatic glove for multimode haptic feedback in reality–virtuality continuum. *Advanced Science* 10, 25 (2023), 2301044.
- [35] Irena Sajovic, Mateja Kert, and Bojana Boh Podgornik. 2023. Smart textiles: A review and bibliometric mapping. *Applied Sciences* 13, 18 (2023), 10489.
- [36] Jialong Shen, Sen Zhang, Xiaomeng Fang, and Sonja Salmon. 2023. Carbonic anhydrase enhanced UV-crosslinked PEG-DA/PEO extruded hydrogel flexible filaments and durable grids for CO<sub>2</sub> capture. *Gels* 9, 4 (2023), 341.
- [37] Kahye Song, Sung Hee Kim, Sungho Jin, Sohyun Kim, Sunho Lee, Jun-Sik Kim, Jung-Min Park, and Youngsu Cha. 2019. Pneumatic actuator and flexible piezoelectric sensor for soft virtual reality glove system. *Scientific reports* 9, 1 (2019), 8988.
- [38] Puchuan Tan, Xi Han, Yang Zou, Xuecheng Qu, Jiangtao Xue, Tong Li, Yiqian Wang, Ruizeng Luo, Xi Cui, Yuan Xi, et al. 2022. Self-powered gesture recognition wristband enabled by machine learning for full keyboard and multicommand input. *Advanced Materials* 34, 21 (2022), 2200793.
- [39] Silvia Terrell, Jesus Miguelafiez, and Antonio Barrientos. 2021. A Soft Haptic Glove Actuated with Shape Memory Alloy and Flexible Stretch Sensors. *Sensors* 21, 16 (2021), 5278. <https://doi.org/10.3390/s21165278>
- [40] Jens Wagner, Hans Winger, Chokri Cherif, and Frank Ellinger. 2023. Smart Glove With Fully Integrated Textile Sensors and Wireless Sensor Frontend for the Tactile Internet. *IEEE Sensors Letters* 7, 2 (2023), 1–4. <https://doi.org/10.1109/LSENS32329991>
- [41] GF West and JC Macnae. 1991. Physics of the electromagnetic induction exploration method. (1991).
- [42] Qiaolian Xie, Qiaoling Meng, Wenwei Yu, Rongna Xu, Zhiyu Wu, Xiaoming Wang, and Hongliu Yu. 2023. Design of a soft bionic elbow exoskeleton based on shape memory alloy spring actuators. *Mechanical Sciences* 14, 1 (2023), 159–170. <https://doi.org/10.5194/ms-14-159-2023>
- [43] Youcan Yan, Zhe Hu, Zhengbao Yang, Wenzhen Yuan, Chaoyang Song, Jia Pan, and Yajing Shen. 2021. Soft magnetic skin for super-resolution tactile sensing with force self-decoupling. *Science Robotics* 6, 51 (2021), eabc8801.
- [44] Ruiyang Yin, Depeng Wang, Shufang Zhao, Zheng Lou, and Guozhen Shen. 2021. Wearable sensors-enabled human–machine interaction systems: from design to application. *Advanced Functional Materials* 31, 11 (2021), 2008936.
- [45] Cheng-Sheng Yu, Chang-Hsien Lin, Yu-Jiun Lin, Shiyang-Yu Lin, Sen-Te Wang, Jenny L Wu, Ming-Hui Tsai, and Shy-Shin Chang. 2020. Clustering heatmap for visualizing and exploring complex and high-dimensional data related to chronic kidney disease. *Journal of Clinical Medicine* 9, 2 (2020), 403.
- [46] Tianhong Catherine Yu, Riki Arakawa, James McCann, and Mayank Goel. 2023. uKit: A Position-Aware Reconfigurable Machine-Knitted Wearable for Gestural Interaction and Passive Sensing using Electrical Impedance Tomography. In *Proceedings of the 2023 CHI Conference on Human Factors in Computing Systems* (Hamburg, Germany) (CHI '23). Association for Computing Machinery, New York, NY, USA, Article 628, 17 pages. <https://doi.org/10.1145/3544548.3580692>
- [47] Hao Yuan, Qirun Zhang, Tong Zhou, Wenbo Wu, Haoran Li, Zhuopeng Yin, Jinning Ma, and Tifeng Jiao. 2024. Progress and challenges in flexible capacitive pressure sensors: Microstructure designs and applications. *Chemical Engineering Journal* 485 (2024), 149926. <https://doi.org/10.1016/j.cej.2024.149926>
- [48] Chao Zhang, Meng Tao, Wei Luo, Xinyuan Zhao, Pei Li, Xin Gou, Zhongyao Li, Chenhui Dong, Chunbao Li, Haofei Shi, and Jun Yang. 2024. Graphene Sterically-Wrapped textile piezoresistive Sensors: A spray coating path for synergistically advancing sensitivity and response range. *Chemical Engineering Journal* 495 (2024), 153533. <https://doi.org/10.1016/j.cej.2024.153533>
- [49] Sen Zhang, Jialong Shen, Peiqi Zhang, Thomas BH Schroeder, Jiahui Chen, Casey Carnevale, Sonja Salmon, and Xiaomeng Fang. 2024. 3D-Printed Hydrogel Filter for Biocatalytic CO<sub>2</sub> Capture. *Advanced Materials Technologies* 9, 19 (2024), 2400025.
- [50] Yufei Zhang, Qiuchun Lu, Jiang He, Zhihao Huo, Runhui Zhou, Xun Han, Mengmeng Jia, Caofeng Pan, Zhong Lin Wang, and Junyi Zhai. 2023. Localizing strain via micro-cage structure for stretchable pressure sensor arrays with ultralow spatial crosstalk. *Nature Communications* 14, 1 (2023), 1252.
- [51] Yin Zhang, XR Wang, and HW Zhang. 2016. Extraordinary galvanomagnetic effects in polycrystalline magnetic films. *Europhysics Letters* 113, 4 (2016), 47003.
- [52] Huichan Zhao, Aftab M Hussain, Ali Israr, Daniel M Vogt, Mihai Duduta, David R Clarke, and Robert J Wood. 2020. A wearable soft haptic communicator based on dielectric elastomer actuators. *Soft robotics* 7, 4 (2020), 451–461.
- [53] Xun Zhao, Yihao Zhou, Jing Xu, Guorui Chen, Yunsheng Fang, Trinny Tat, Xiao Xiao, Yang Song, Song Li, and Jun Chen. 2021. Soft fibers with magnetoelasticity for wearable electronics. *Nature communications* 12, 1 (2021), 6755.
- [54] Yihao Zhou, Xun Zhao, Jing Xu, Yunsheng Fang, Guorui Chen, Yang Song, Song Li, and Jun Chen. 2021. Giant magnetoelastic effect in soft systems for bioelectronics. *Nature Materials* 20, 12 (2021), 1670–1676.
- [55] Erhan Zhuo, Ziwen Wang, Xiaochen Chen, Junhao Zou, Yuan Fang, Jiekai Zhuo, and Yicheng Li. 2023. Wearable Smart Fabric Based on Hybrid E-Fiber Sensor for Real-Time Finger Motion Detection. *Polymers* 15, 13 (2023), 2934. <https://doi.org/10.3390/polym15132934>